

# Sparse Estimation using Bayesian Hierarchical Prior Modeling for Real and Complex Models

Niels Lovmand Pedersen\*, Dmitriy Shutin<sup>†</sup>, Carles Navarro Manchón\*, Bernard Henri Fleury\*

\*Department of Electronic Systems, Aalborg University

Niels Jernes Vej 12, DK-9220 Aalborg, Denmark, Email: {nlp,cnm,bfl}@es.aau.dk

<sup>†</sup>Department of Electrical Engineering, Princeton University

E-QUAD B311, Olden Street, Princeton, 08544 NJ, USA, Email: dshutin@princeton.edu

## Abstract

Sparse modeling and estimation of complex signals is not uncommon in practice. However, historically, much attention has been drawn to real-valued system models, lacking the research of sparse signal modeling and estimation for complex-valued models. This paper introduces a unifying sparse Bayesian formalism that generalizes to complex- as well as real-valued systems. The methodology relies on hierarchical Bayesian sparsity-inducing prior modeling of the parameter of interest. This approach allows for the Bayesian modeling of  $\ell_1$ -norm constraint for complex-valued as well as real-valued models. In addition, the proposed two-layer hierarchical model allows for the design of novel priors for sparse estimation that outperform the Bayesian formulation of the  $\ell_1$ -norm constraint and lead to estimators approximating a soft-thresholding rule. An extension of the two-layer model to a three-layer model is also presented. Varying the free parameters of the three-layer model leads to estimators that approximate a hard-thresholding rule. Finally, a variational message-passing (VMP) implementation of the proposed Bayesian method that effectively exploits the hierarchical structure of the inference problem is presented. The simulation results show that the VMP algorithm outperforms existing sparse methods both in terms of the sparsity of the estimation results and achieved mean squared error in low and moderate SNR regimes.

This work was supported in part by the 4GMCT cooperative research project funded by Intel Mobile Communications, Agilent Technologies, Aalborg University and the Danish National Advanced Technology Foundation. This research was also supported in part by the project ICT- 248894 Wireless Hybrid Enhanced Mobile Radio Estimators (WHERE2) and by Erwin Schrödinger Postdoctoral Fellowship, Austrian Science Fund (FWF) Project J2909-N23.

This work has been submitted to the IEEE for possible publication. Copyright may be transferred without notice, after which this version may no longer be accessible.

## I. INTRODUCTION

During the last decade the research on compressive techniques and sparse signal representations has received considerable attention (see e.g., [1]–[4]). With a few minor variations, the general goal of sparse reconstruction is to estimate the parameter vector  $\alpha$  of the following canonical model:

$$\mathbf{y} = \mathbf{H}\alpha + \mathbf{w}. \quad (1)$$

In this expression  $\mathbf{y}$  is a  $M \times 1$  vector of measurement samples,  $\mathbf{H} = [\mathbf{h}_1, \dots, \mathbf{h}_L]$  is an  $M \times L$  measurement matrix with  $L$  column vectors  $\mathbf{h}_l$ . The additive term  $\mathbf{w}$  is an  $M \times 1$  perturbation vector, which is assumed to be a white Gaussian random vector with zero-mean and covariance matrix  $\Sigma = \lambda^{-1}\mathbf{I}$  with  $\lambda > 0$  being the noise precision parameter. The unknown  $L \times 1$  parameter vector  $\alpha = [\alpha_1, \dots, \alpha_L]^T$  has only  $K$  non-zero entries, i.e.,  $\alpha$  is assumed to be  $K$ -sparse. System model (1) can be either real-valued, when  $\mathbf{H}$  and  $\mathbf{w}$  are real and  $\alpha$  is real [1], [2], or complex-valued, when  $\mathbf{H}$  or  $\mathbf{w}$  is complex and  $\alpha$  is complex as well.

Historically, a real-valued system model has dominated the research in sparse signal reconstruction and compressive sampling techniques. However, complex systems are not so uncommon in practice in which sparse parameter estimation is sought as well. An example is the estimation of the dominant multipath components in the response of wireless channels [4], [5]. Motivated by the lack of formal tools for sparse learning in complex-valued system models and inspired by the recent developments of sparse Bayesian methods [3], [6]–[11] we propose a unifying sparse Bayesian formalism that applies to both real- and complex-valued system models. The formalism enables to generalize and improve the sparse Bayesian methods proposed nowadays.

Sparse Bayesian learning (SBL) [3], [12], [13] applied to model (1) aims at finding a sparse *maximum a posteriori* (MAP) estimate of  $\alpha$

$$\hat{\alpha}_{\text{MAP}} = \underset{\alpha}{\operatorname{argmin}} \left\{ \rho \|\mathbf{y} - \mathbf{H}\alpha\|_2^2 + \lambda^{-1}Q(\alpha) \right\}, \quad (2)$$

with  $\rho = 1/2$  (real model) or  $\rho = 1$  (complex model), the Euclidean norm  $\|\cdot\|_2$ , and the penalty term  $Q(\alpha) \propto e^{-\log p(\alpha)}$ ,<sup>1</sup> by modeling the prior  $p(\alpha)$  using a hierarchical structure, which involves a conditional prior  $p(\alpha|\gamma)$  and a hyperprior  $p(\gamma)$ . The hierarchical approach to the representation of sparsity-inducing prior has several important advantages. First of all, one is free to choose the prior pdfs in the formulation of the hierarchical structure, which is advantageous for the generalization of

<sup>1</sup> $x \propto^e y$  denotes  $\exp(x) = \exp(\beta) \exp(y)$  and thus  $x = \beta + y$  for some arbitrary constant  $\beta$ .

SBL for complex- and real-valued system models. When carefully chosen, the resulting hierarchical structure also allows for the construction of efficient inference algorithms, in terms of sparsity enhancing capability, and an analytical derivation of the inference expressions. Second, the two-layer hierarchy can be naturally extended with an additional hierarchy tier by treating the parameters of the hyperprior – the hyperparameters – as random variables specified by a hyper-hyperprior distribution. This yields additional degrees of freedom in controlling the sparsity properties of the resulting inference scheme, as will be demonstrated later in this work.

The SBL methodology has developed following two distinct approaches that differ in the way the hierarchical prior model is constructed. The first approach is exemplified by the relevance vector machines (RVMs) [12]. In RVM, each component of  $\alpha$  is independently constrained using a two-layer hierarchical prior  $p(\alpha_l|\gamma_l)p(\gamma_l)$ , where  $p(\alpha_l|\gamma_l)$  is a Gaussian probability density function (pdf) with zero-mean and variance  $\gamma_l$ , and  $p(\gamma_l) \equiv p(\gamma_l; a_l, b_l) = b_l^{a_l} \gamma_l^{-a_l-1} \exp(-b_l/\gamma_l)/\Gamma(a_l)$  is an inverse gamma hyperprior pdf with parameters  $a_l$  and  $b_l$ .<sup>2</sup> Further in the text we refer to this formulation of the hierarchical prior pdf as a Gaussian-Inverse gamma (G-IGa) prior model. Notice that the G-IGa prior model applies equally well to the modeling of complex-valued as well as real-valued  $\alpha_l$ . Using the G-IGa prior model an RVM algorithm is then formulated to estimate the hyperparameters  $\gamma = [\gamma_1, \dots, \gamma_L]^T$  by maximizing its posterior pdf  $p(\gamma|\mathbf{y}, \lambda) \propto p(\gamma) \int p(\mathbf{y}|\alpha, \lambda)p(\alpha|\gamma)d\alpha$ ; as  $\gamma_l$  decreases it drives the corresponding weight  $\alpha_l$  towards zero, thus encouraging a solution with only a few non-zero coefficients in  $\alpha$ . It is known [12] that the prior  $p(\alpha) = \int p(\alpha, \gamma)d\gamma$  is the product of pdfs of Student-t distributions over  $\alpha_l$ . Under such a prior most of the probability mass is concentrated along the coordinate axes in the parameter space, thus encouraging a posterior distribution with a mode lying close to these axes in the  $\alpha$ -space [13]. The analytical tractability of the resulting inference problem allows for a further analysis of SBL with these hierarchical priors, especially in case of a non-informative hyperprior  $p(\gamma) \propto \prod_{l=1}^L \gamma_l^{-1}$ , which is also termed automatic relevance determination (ARD) [11], [12]. In the latter case the prior  $p(\alpha)$  is improper:  $p(\alpha) \propto \prod_{l=1}^L 1/|\alpha_l|$ . It leads to the log-sum penalization term  $Q(\alpha) = \sum_{l=1}^L \log |\alpha_l|$  in (2), which is known to strongly promote sparsity [7], [8].<sup>3</sup> Furthermore, ARD leads to very efficient and fast inference schemes [6], [14], [15].

The second approach to SBL was proposed in [16] for real-valued models to realize a popular  $\ell_1$ -

<sup>2</sup>In the original formulation of the RVM algorithm the parameter  $\gamma_l$  models the precision (inverse variance) of the conditional Gaussian prior  $p(\alpha_l|\gamma_l)$  and the hyperprior  $p(\gamma_l; a_l, b_l)$  is a gamma pdf. The model has been reformulated here to match the framework adopted in this sequel of the paper.

<sup>3</sup>Note, however, that the hierarchical formulation realizes this log-sum penalty term indirectly through the product of two pdfs that form a conjugate family.

norm regularization for each component of  $\alpha$ . This approach consists in independently constraining each element of  $\alpha$  using a two-layer hierarchical prior  $p(\alpha_l|\gamma_l)p(\gamma_l)$ . Similarly to the G-IGa model  $p(\alpha_l|\gamma_l)$  is a Gaussian pdf with zero-mean and variance  $\gamma_l$ ; however, the hyperprior  $p(\gamma_l) \equiv p(\gamma_l; \eta)$  is selected as an exponential pdf with rate parameter  $\eta$ . We refer to this formulation of the hierarchical prior pdf as a Gaussian-exponential (G-E) prior model. It can be shown [16] that in this case the prior pdf  $p(\alpha; \eta) = \int p(\alpha|\gamma)p(\gamma; \eta)d\gamma \propto \prod_{l=1}^L \exp(-\sqrt{2\eta}|\alpha_l|)$  is the product of Laplace pdfs with zero-mean and scale parameter  $\sqrt{2\eta}$ . In this case the penalty term in (2) reads  $Q(\alpha) = \sqrt{2\eta}\|\alpha\|_1$  with  $\|\cdot\|_1$  denoting the  $\ell_1$ -norm. The MAP estimate with this selection of  $Q(\alpha)$  is called Least Absolute Shrinkage and Selection Operator (LASSO) [17]. The popularity of the LASSO regression is mainly attributed to the convexity of the  $\ell_1$  penalty term  $Q(\alpha) = \sqrt{2\eta}\|\alpha\|_1$  as well as to its provable sparsity-inducing properties (see, e.g., [2], [18]).

The sparsity properties of the LASSO estimator depend heavily on the value of the regularization parameter  $\kappa = \lambda^{-1}\sqrt{2\eta}$ . If  $\kappa$  is selected too large, the resulting estimator produces overly sparse estimates, i.e., relevant information will be discarded; in contrast, small values of  $\kappa$  lead to non-sparse solutions, especially in low signal-to-noise ratio (SNR) regime. While techniques exist for empirically choosing the regularization parameters [8], the Bayesian methodology provides all the tools necessary for finding an optimal regularization term. In other words, by modeling  $\eta$  and  $\lambda$  as random variables and incorporating them into the inference framework, an optimal value of  $\kappa$  can be found. This requires extending the two-layer prior modeling of  $p(\alpha)$  with a third layer — the “hyper-hyperprior” pdf for  $\eta$ . Naturally, the “hyper-hyperprior” again depends on some parameters that have to be specified. However, it is reasonable to assume that the performance of the resulting estimator is less sensitive to the exact choice of these “hyper-hyperparameters”: the tiers of such hierarchical priors can be seen as different layers of abstraction from the actual model parameter vector  $\alpha$ . Thus, on the highest layer such a “hyper-hyperprior” gives a very abstract description of the representation of  $\alpha$ . In this work we propose several extensions and generalizations of this hierarchical modeling approach.

Our goal in this work is threefold. First, we extend the G-E prior model to complex domain, effectively generalizing the hierarchical prior formulation for real as well as complex models. We do so by using a gamma hyperprior  $p(\gamma_l; \epsilon, \eta_l)$  instead of an exponential prior; furthermore,  $L$  individual parameters  $\eta_l$  are used instead of a single regularization parameter. We will refer to this new hierarchical prior formulation as Gaussian-gamma (G-Ga) prior model. The obtained results naturally generalize those obtained in [16] for real  $\alpha$ . We demonstrate that by varying the shape parameter  $\epsilon$  of the gamma hyperprior  $p(\gamma_l; \epsilon, \eta_l)$  a family of solutions for  $\alpha$  that approximate a soft-thresholding rule with different degrees of sparseness

is obtained. Second, instead of a two-layer prior we propose a three-layer hierarchical prior for both real and complex parameters. This is realized by modeling the hyperprior parameters  $\eta_l$  as random variables with the gamma pdf  $p(\eta_l) \equiv p(\eta_l; a_l, b_l) = b_l^{a_l} \eta_l^{a_l-1} \exp(-b_l \eta_l) / \Gamma(a_l)$ . This leads to a model with  $2L+1$  free parameters, i.e.,  $\epsilon$  and  $a_l, b_l, l = 1, \dots, L$ , to control the degree of sparseness of the resulting solution. We show that, in contrast to the G-Ga model, varying the parameter  $\epsilon$  with fixed  $a_l$  and  $b_l$  leads in this case to a family of solutions for  $\alpha$  that approximate a hard-thresholding rule. Moreover, a weakly informative prior can be constructed that induces an equivalent weighted log-sum penalization of the parameter likelihood function [8], [10]. This three-layer prior model we term Gaussian-gamma-gamma (G-Ga-Ga) prior model. Furthermore, we show that for both two-layer and three-layer prior models, choosing non-informative hyperpriors yields a log-sum penalization of the parameter likelihood, which is identical to the ARD formulation of the RVM-type of hierarchical prior. Finally, we propose a variational Bayesian message passing algorithm that exploits the hierarchical structure of the inference problem. Due to the adopted choice of the pdfs in the hierarchical prior model it is possible to compute the messages in closed form. Thus, inference can be implemented very efficiently. We should mention that a three-layer prior model has been also independently proposed in [7] for hierarchical adaptive LASSO (HAL). In [7] the authors use a three-layer hierarchical prior to motivate the adaptive version of the LASSO estimator. There are, however, several important distinctions between their approach and the one advocated in our work. First of all, although a three-layer hierarchy is used, the prior pdfs used in the hierarchy prohibit an application of this structure to models with complex parameters; specifically, one does not obtain a LASSO-type of objective function when this hierarchical modeling is applied to models with complex parameters. Second, the inference algorithm does not really exploit the three-layer hierarchy. Instead, it works with a two-layer structure, where the first layer is a Laplace pdf and the second layer is a gamma pdf. Such a two-layer structure has been explicitly used earlier for sparse estimation of multipath wireless channels in [5]. More on this will be discussed later in the text.

Throughout this paper we shall make use of the following notation. For vectors  $\mathbf{x}$  and matrices  $\mathbf{X}$ ,  $(\cdot)^T$  and  $(\cdot)^H$  denote respectively the transpose and the Hermitian transpose. The expression  $\langle f(\mathbf{x}) \rangle_{q(\mathbf{x})}$  denotes the expectation of a function  $f(\mathbf{x})$  with respect to a density  $q(\mathbf{x})$ . For a random vector  $\mathbf{x}$ ,  $\text{N}(\mathbf{x}|\mathbf{a}, \mathbf{B})$  and  $\text{CN}(\mathbf{x}|\mathbf{a}, \mathbf{B})$  denote respectively a multivariate real and a multivariate complex Gaussian pdf with a mean  $\mathbf{a}$  and a covariance matrix  $\mathbf{B}$ ; similarly,  $\text{Ga}(x|a, b) = \frac{b^a}{\Gamma(a)} x^{a-1} \exp(-bx)$  denotes a Gamma pdf with shape parameter  $a$  and rate parameter  $b$ . The range of integration of integrals will not be explicitly given when it is obvious.

## II. BAYESIAN FRAMEWORK FOR SPARSE ESTIMATION

We begin with the specification of the probabilistic structure of the SBL problem for model (1). Two types of hierarchical prior models for  $\alpha$  are considered: a two-layer and a three-layer hierarchical model. Later we will see that these models lead to priors for  $\alpha$  with distinct sparsity-inducing properties.

The joint pdf of system model (1) with a two-layer prior model for  $\alpha$  reads

$$p(\mathbf{y}, \alpha, \gamma, \lambda) = p(\mathbf{y}|\alpha, \lambda)p(\lambda)p(\alpha|\gamma)p(\gamma). \quad (3)$$

The joint pdf of system model (1) with a three-layer prior model for  $\alpha$  is obtained by assuming that the parameters  $\eta$  of the  $p(\gamma)$  in (3) are random. The resulting joint pdf is then specified as

$$p(\mathbf{y}, \alpha, \gamma, \eta, \lambda) = p(\mathbf{y}|\alpha, \lambda)p(\lambda)p(\alpha|\gamma)p(\gamma|\eta)p(\eta). \quad (4)$$

Both the two-layer formulation (3) and the three-layer formulation (4) share the same likelihood function  $p(\mathbf{y}|\alpha, \lambda)$  and the prior pdf of the noise precision parameter  $p(\lambda)$ . Due to (1) the likelihood function is Gaussian:  $p(\mathbf{y}|\alpha, \lambda) = \mathcal{N}(\mathbf{y}|\mathbf{H}\alpha, \lambda^{-1}\mathbf{I})$  for the real-valued system model and  $p(\mathbf{y}|\alpha, \lambda) = \mathcal{CN}(\mathbf{y}|\mathbf{H}\alpha, \lambda^{-1}\mathbf{I})$  for the complex-valued model. The prior  $p(\lambda)$  is selected as a gamma prior, i.e.,  $p(\lambda) = p(\lambda; c, d) \triangleq \text{Ga}(\lambda|c, d)$ . This choice is convenient since the gamma distribution is a conjugate prior for the precision of a Gaussian likelihood function. Additionally, selecting  $c = d = 0$  makes this prior non-informative.

Let us specify the structure of the hierarchical priors of  $\alpha$  in (3) and (4). Motivated by [12], [16] we select the conditional prior  $p(\alpha|\gamma) = \prod_{l=1}^L p(\alpha_l|\gamma_l)$  to be the product of Gaussian pdfs. While in [12], [16] real-valued  $\alpha$  was considered, here we consider both real- and complex-valued  $\alpha$ . To this end we define

$$p(\alpha_l|\gamma_l) = \left( \frac{\rho}{\pi\gamma_l} \right)^\rho \exp \left( -\rho \frac{|\alpha_l|^2}{\gamma_l} \right) \quad (5)$$

with the parameter  $\rho \in \{\frac{1}{2}, 1\}$ . The conditional prior  $p(\alpha_l|\gamma_l)$  for real-valued  $\alpha_l$  is realized by selecting  $\rho = 1/2$ , while  $\rho = 1$  entails the prior for complex-valued  $\alpha_l$ . In the next section we compute the prior for  $\alpha$  that results from the two-layer prior model and analyze its sparsity-inducing property. We redo the same exercise in the following section with the three-layer prior model.

### A. Two-Layer Hierarchical Prior Model

As we have already mentioned, the original G-E prior model in [16] assumes that  $p(\gamma)$  is a product of exponential pdfs with a common rate parameter  $\eta$ . We can easily generalize this model by considering  $p(\gamma)$  as a product of gamma pdfs with individual rate parameters. Specifically, we assume that  $p(\gamma) = \prod_{l=1}^L p(\gamma_l)$  with  $p(\gamma_l) = p(\gamma_l; \epsilon, \eta_l) \triangleq \text{Ga}(\gamma_l | \epsilon, \eta_l)$ . The G-E prior model is then the special case with the settings  $\epsilon = 1$  and  $\eta_1 = \dots = \eta_L = \eta$ . We define now  $\boldsymbol{\eta} = [\eta_1, \dots, \eta_L]^T$  and compute the prior of  $\boldsymbol{\alpha}$  to be

$$p(\boldsymbol{\alpha}; \epsilon, \boldsymbol{\eta}) = \int_0^\infty p(\boldsymbol{\alpha} | \boldsymbol{\gamma}) p(\boldsymbol{\gamma}; \epsilon, \boldsymbol{\eta}) d\boldsymbol{\gamma} = \prod_{l=1}^L p(\alpha_l; \epsilon, \eta_l) \quad (6)$$

with

$$p(\alpha_l; \epsilon, \eta_l) = \frac{2\rho^{\frac{(\epsilon+\rho)}{2}}}{\pi^\rho \Gamma(\epsilon)} \eta_l^{\frac{(\epsilon+\rho)}{2}} |\alpha_l|^{\epsilon-\rho} K_{\epsilon-\rho}(2\sqrt{\rho\eta_l} |\alpha_l|). \quad (7)$$

In this expression,  $K_\nu(\cdot)$  is the modified Bessel function of the second kind and order  $\nu \in \mathbb{R}$ . Further in the text we refer to this formulation of the hierarchical prior pdf as Gaussian-gamma (G-Ga) prior model. The prior (7) is valid for real-valued ( $\rho = 1/2$ ) as well as for complex-valued ( $\rho = 1$ )  $\alpha_l$ .

By selecting  $\epsilon = 1$ ,  $\rho = 1/2$ , and using the identity  $K_{\frac{1}{2}}(z) = \sqrt{\frac{\pi}{2z}} \exp(-z)$  [19], (7) yields the Laplace prior for real  $\alpha_l$ :

$$p(\alpha_l; \epsilon = 1, \eta_l) = \sqrt{\frac{\eta_l}{2}} \exp(-\sqrt{2\eta_l} |\alpha_l|), \quad \alpha_l \in \mathbb{R}. \quad (8)$$

In the complex case, when  $\rho = 1$ , it is easy to see that selecting  $\epsilon = 3/2$  leads to the same order of the Bessel function in (7) as in the real case. Making use of the same identity for the Bessel function we find the corresponding prior for complex  $\alpha_l$ :

$$p(\alpha_l; \epsilon = 3/2, \eta_l) = \frac{2\eta_l}{\pi} \exp(-2\sqrt{\eta_l} |\alpha_l|), \quad \alpha_l \in \mathbb{C}. \quad (9)$$

Hence, the G-Ga prior model realizes the  $\ell_1$  penalty term  $Q(\boldsymbol{\alpha}; \boldsymbol{\eta}) = 2 \sum_{l=1}^L \sqrt{\rho\eta_l} |\alpha_l|$  with  $\epsilon = 1$  for real  $\boldsymbol{\alpha}$  and with  $\epsilon = 3/2$  for complex  $\boldsymbol{\alpha}$ .

The G-Ga prior model can be used with arbitrary values of  $\epsilon$ , leading to the general optimization problem (2) with

$$Q(\boldsymbol{\alpha}; \epsilon, \boldsymbol{\eta}) = \sum_{l=1}^L \log \left( |\alpha_l|^{\epsilon-\rho} K_{\epsilon-\rho}(2\sqrt{\rho\eta_l} |\alpha_l|) \right). \quad (10)$$

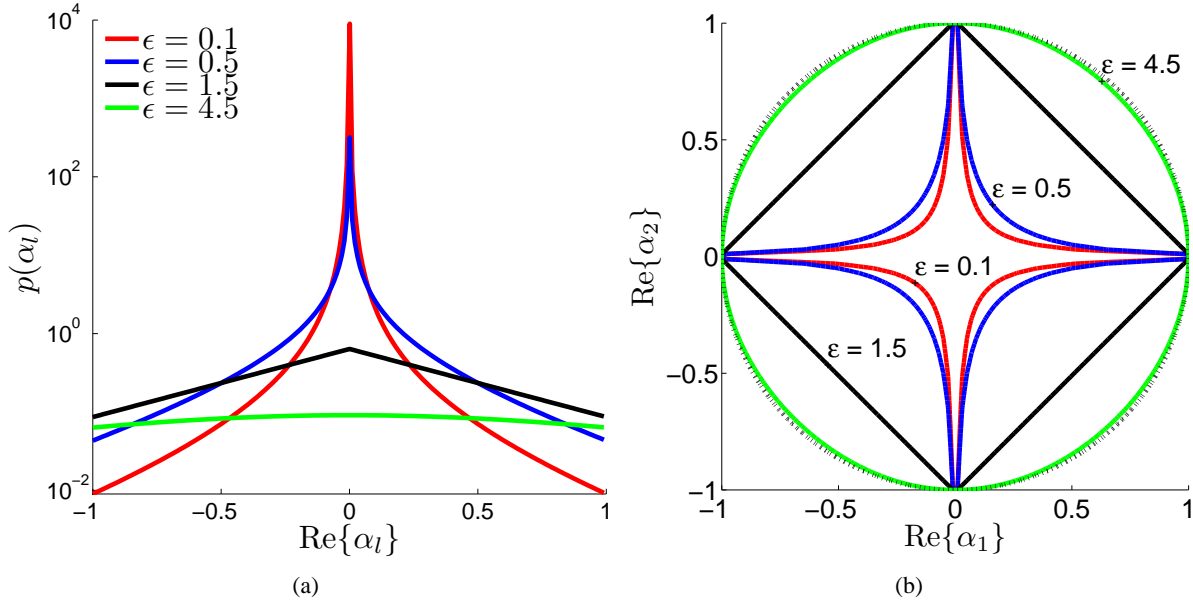


Fig. 1. Two-layer hierarchical prior pdf for the complex system model with the setting  $\eta = 1$ : (a) The restriction to  $\mathbb{R}(\text{Im}\{\alpha_l\} = 0)$  of  $p(\alpha_l; \epsilon, \eta)$  (7) for different values of  $\epsilon$ . (b) Contour plot of the restriction to the  $\text{Im}\{\alpha_1\} = \text{Im}\{\alpha_2\} = 0$  — plane of  $Q(\alpha_1, \alpha_2; \epsilon, \eta) \propto e^{-\log p(\alpha_1; \epsilon, \eta)p(\alpha_2; \epsilon, \eta)}$ . In (b) the black dashed line indicates the penalty term resulting when the prior pdf is a circular symmetric Gaussian pdf.

One important observation is that decreasing  $\epsilon$  beyond  $3/2$  in the complex case (or equivalently beyond  $1$  in the real case) leads to a non-convex penalty term that resembles the  $\ell_p$ -norm penalty for  $0 < p < 1$ .<sup>4</sup> Unfortunately, in this case the optimization problem (2) with penalty term (10) is no longer convex. Note, however, that the hierarchical approach advocated in this work does not involve a direct optimization of the objective function in (2). Instead, the non-convex penalty term (10) is realized indirectly as a product of Gaussian and gamma pdfs. Moreover, since in the G-Ga model formulation the prior  $p(\alpha|\gamma)$  is Gaussian, the resulting MAP objective function for  $\alpha$  is necessarily convex with respect to  $\alpha$  irrespective of the value of  $\epsilon$ .<sup>5</sup>

Let us stress that (6) represents a family of prior pdfs for  $\alpha$  parameterized by  $\epsilon$  and  $\eta$ . While the entries in  $\eta$  can be recognized as multiple regularization parameters, the impact of  $\epsilon$  is less straightforward. To better understand its influence on the shape of (6) we visualize in Fig. 1(a) the restriction<sup>6</sup> to  $\mathbb{R}$  of the prior  $p(\alpha_l, \epsilon, \eta_l)$  in (7) with  $\rho = 1$  for various values of  $\epsilon$ . Observe the change of the shape of  $p(\alpha_l; \epsilon, \eta_l)$

<sup>4</sup>The norm  $\ell_p$ ,  $0 < p < 1$ , better approximates the pseudo-norm  $\ell_0$  — the number of non-zero entries in the vector — as compared to  $\ell_p$  with  $p \geq 1$ .

<sup>5</sup>The same is true for G-E and G-IGa models.

<sup>6</sup>Let  $f$  denote a function defined on a set  $A$ . The restriction of  $f$  to a subset  $B \subset A$  is the function defined on  $B$  that coincides with  $f$  on this subset.

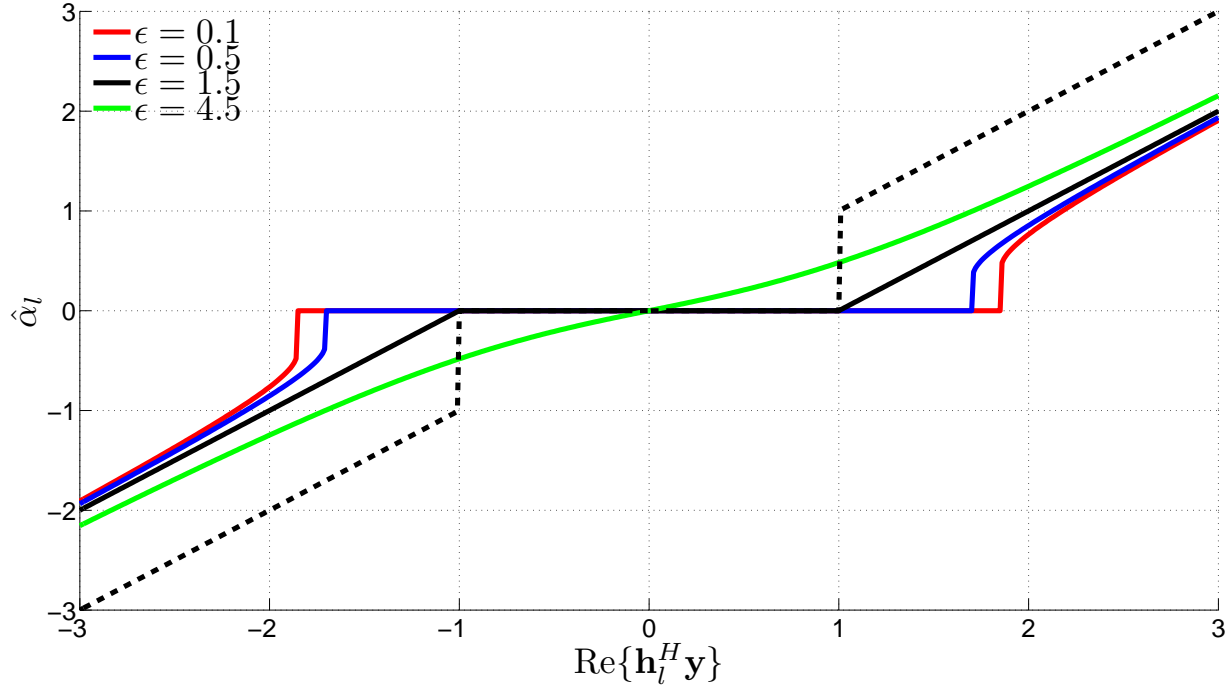


Fig. 2. Two-layer hierarchical prior for the complex system model: Restriction to  $\text{Im}\{\mathbf{h}_l^H \mathbf{y}\} = 0$  of the resulting MAP estimation rule (2) with  $\epsilon$  as a parameter in the case when  $\mathbf{H}$  is orthonormal. The black dashed line indicates the hard-threshold rule [20].

with  $\epsilon$ : the smaller the value of  $\epsilon$  the more rapidly  $p(\alpha_l, \epsilon, \eta_l)$  decays around the origin. In Fig. 1(b) we show the contour lines of the restriction to  $\mathbb{R}$  of  $Q(\alpha_1, \alpha_2; \epsilon, \eta) \propto e^{-\log p(\alpha_1; \epsilon, \eta)p(\alpha_2; \epsilon, \eta)}$ ; each contour line is computed for a specific choice of  $\epsilon$ . It can be seen from the plots that as  $\epsilon$  decreases towards 0 more probability mass concentrates along the  $\alpha$ -axes; as a consequence, the mode of the resulting posterior is more likely to be found close to the axes, thus indicating a sparse solution. The behavior of the classical  $\ell_1$  penalty term obtained for  $\epsilon = 3/2$  can also be clearly recognized.

In order to get further insight into the impact of  $\epsilon$  on the MAP estimate  $\hat{\alpha}$  with penalty term (10), we consider the case when  $\mathbf{H}$  is orthonormal, i.e., when  $\mathbf{h}_l^H \mathbf{h}_k = \delta_{k,l}$ , where  $\delta_{k,l}$  is the Kronecker delta. In this case the solution  $\hat{\alpha}$  can be easily computed since the optimization (2) decouples into  $L$  independent scalar optimization problems. Furthermore, when the G-Ga prior model realizes an  $\ell_1$ -norm constraint, i.e., the prior pdfs (8) (real case) or (9) (complex case) is selected, the MAP solution can even be computed analytically as follows:

$$\hat{\alpha}_l = \text{sign}(\mathbf{h}_l^H \mathbf{y}) \max \left\{ 0, |\mathbf{h}_l^H \mathbf{y}| - \lambda^{-1} \sqrt{\frac{\eta_l}{\rho}} \right\}, \quad l = 1, \dots, L, \quad (11)$$

where  $\text{sign}(x) = x/|x|$ . The interpretation of this result is quite intuitive: for complex  $\alpha_l$  the region where the estimate  $\hat{\alpha}_l$  is exactly zero is the closed disc with radius  $\lambda^{-1}\sqrt{\eta_l}$  centered at origin; for real  $\alpha_l$  it is given by the closed interval  $[-\lambda^{-1}\sqrt{2\eta_l}, \lambda^{-1}\sqrt{2\eta_l}]$ . Correspondingly, the solution (11) is a soft-thresholding rule for each entry in  $\hat{\alpha}$  with threshold  $\lambda^{-1}\sqrt{\frac{\eta_l}{\rho}}$ . In Fig. 2 we visualize the estimation rules produced by the MAP solver for different values of  $\epsilon$ . Note their typical soft-threshold-like behavior. As  $\epsilon \rightarrow 0$ , more components of  $\hat{\alpha}$  are pulled towards zero since the threshold value increases, thus encouraging a sparser solution.

### B. Three-Layer Hierarchical Prior Model

We now turn to the SBL problem with a three-layer prior model for  $\alpha$  represented by the joint pdf in (4). Specifically, we extend the G-Ga prior model to a three-layer model by considering the hyperparameters in  $\eta$  as random. We assume that  $p(\eta) = \prod_l^L p(\eta_l)$ , where  $p(\eta_l) = p(\eta_l; a_l, b_l) \triangleq \text{Ga}(\eta_l | a_l, b_l)$ . The resulting three-layer model we term Gaussian-gamma-gamma (G-Ga-Ga) prior model.

Let us now compute the prior  $p(\alpha)$  that corresponds to the G-Ga-Ga model. First, we note that  $p(\alpha, \gamma, \eta) = p(\alpha|\gamma)p(\gamma|\eta)p(\eta) = \prod_{l=1}^L p(\alpha_l|\gamma_l)p(\gamma_l|\eta_l)p(\eta_l)$  and marginalize  $p(\alpha, \gamma, \eta)$  over  $\eta$ . This requires computing  $p(\alpha|\gamma)p(\gamma) = p(\alpha|\gamma) \int p(\gamma|\eta)p(\eta)d\eta$ . Defining  $\mathbf{a} \triangleq [a_1, \dots, a_L]^T$  and  $\mathbf{b} \triangleq [b_1, \dots, b_L]^T$  we obtain

$$p(\gamma; \epsilon, \mathbf{a}, \mathbf{b}) = \prod_l^L \int_0^\infty p(\gamma_l|\eta_l; \epsilon)p(\eta_l; a_l, b_l)d\eta_l = \prod_l^L p(\gamma_l; \epsilon, a_l, b_l), \quad (12)$$

where

$$p(\gamma_l; \epsilon, a_l, b_l) = \frac{b_l^{a_l} \Gamma(\epsilon + a_l)}{\Gamma(\epsilon) \Gamma(a_l)} \gamma_l^{\epsilon-1} (\gamma_l + b_l)^{-(\epsilon+a_l)}. \quad (13)$$

Finally, marginalizing  $p(\alpha|\gamma)p(\gamma; \epsilon, \mathbf{a}, \mathbf{b})$  over  $\gamma$  yields

$$p(\alpha; \epsilon, \mathbf{a}, \mathbf{b}) = \prod_l^L p(\alpha_l; \epsilon, a_l, b_l) \quad (14)$$

with

$$\begin{aligned} p(\alpha_l; \epsilon, a_l, b_l) &= \int_0^\infty p(\alpha_l|\gamma_l)p(\gamma_l)d\gamma_l \\ &= \left( \frac{\rho}{\pi b_l} \right)^\rho \frac{\Gamma(\epsilon + a_l)\Gamma(a_l + \rho)}{\Gamma(\epsilon)\Gamma(a_l)} \left( \rho \frac{|\alpha_l|^2}{b_l} \right)^{\epsilon-\rho} U\left(\epsilon + a_l; \epsilon - \rho + 1; \rho \frac{|\alpha_l|^2}{b_l}\right). \end{aligned} \quad (15)$$

In this expression,  $U(\cdot; \cdot; \cdot)$  is the confluent hypergeometric function [19]. Unfortunately, this function

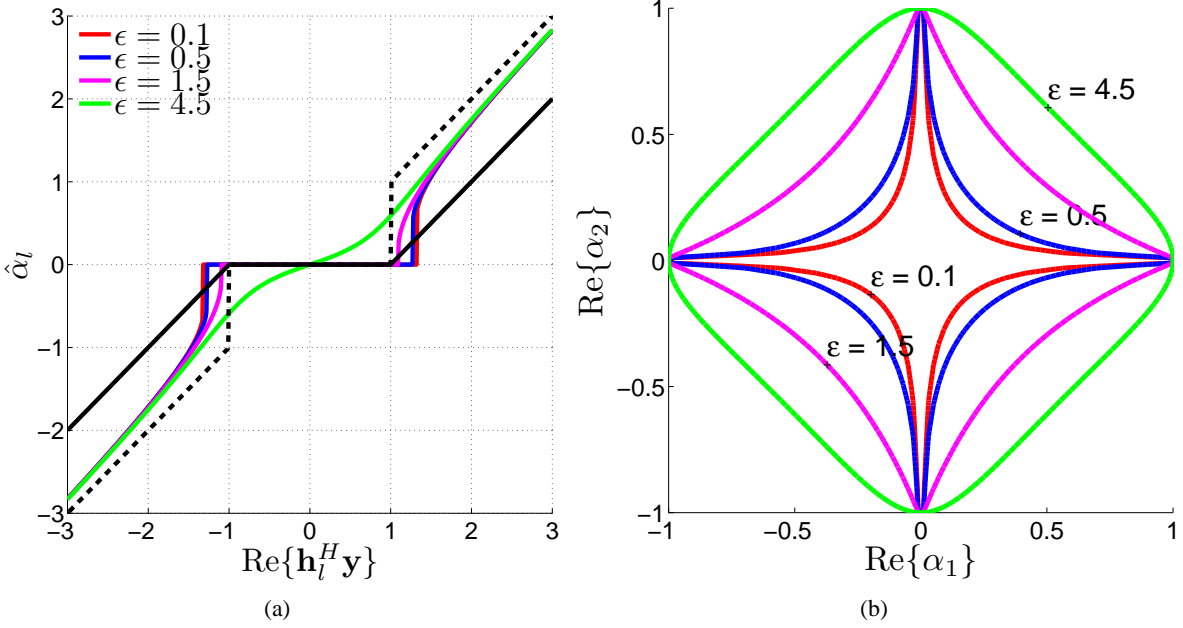


Fig. 3. Three-layer hierarchical prior pdf for the complex system model with the setting  $a = 1$ ,  $b = 0.1$ : (a) Restriction to  $\text{Im}\{\mathbf{h}_l^H \mathbf{y}\} = 0$  of the resulting MAP estimation rule (2) with  $\epsilon$  as a parameter in the case when  $\mathbf{H}$  is orthonormal. The black dashed line indicates the hard-threshold rule and the black solid line the soft-threshold rule (11). (b) Contour plot of the restriction to the  $\text{Im}\{\alpha_1\} = \text{Im}\{\alpha_2\} = 0$  plane of the penalty term  $Q(\alpha_1, \alpha_2; \epsilon, a, b) \propto e^{-\log p(\alpha_1; \epsilon, a, b)p(\alpha_2; \epsilon, a, b)}$ .

makes a further analytical investigation of (15) rather difficult. Nonetheless, we can study its behavior numerically. Following the same approach as for the G-Ga prior model, we show the estimation rules produced by the MAP solver for different values of  $\epsilon$  and fixed parameters  $a_l$  and  $b_l$  when  $\mathbf{H}$  is orthonormal in Fig. 3(a). Notice, the estimation rules obtained with the G-Ga-Ga prior model approximate the hard-thresholding rule. In Fig. 3(b), we depict the contour of the penalty term  $Q(\alpha_1, \alpha_2; \epsilon, a, b) \propto e^{-\log p(\alpha_1; \epsilon, a, b)p(\alpha_2; \epsilon, a, b)}$ . Observe that although the contours are qualitatively similar to those shown in Fig. 1(b) for the G-Ga model, the corresponding estimation rules in Fig. 3(a) are not.

### C. Weighted log-sum Penalization

The use of the additional third layer in the G-Ga-Ga prior model leads to the introduction of the additional free parameter vectors  $\mathbf{a}$  and  $\mathbf{b}$  which must be selected in addition to the prior parameter  $\epsilon$ . In this section we discuss a selection of these parameters that leads to a “weakly” informative prior for  $\boldsymbol{\alpha}$  with good sparsity-inducing properties.

Recall that the entries in  $\boldsymbol{\eta}$  in the G-Ga prior model represent regularization parameters. The range of appropriate values for  $\boldsymbol{\eta}$  is primarily determined by the particular SNR, measurement signal  $\mathbf{y}$ , and dictionary  $\mathbf{H}$  (see (11)); this range can be quite large in general. Thus, it makes sense to employ a

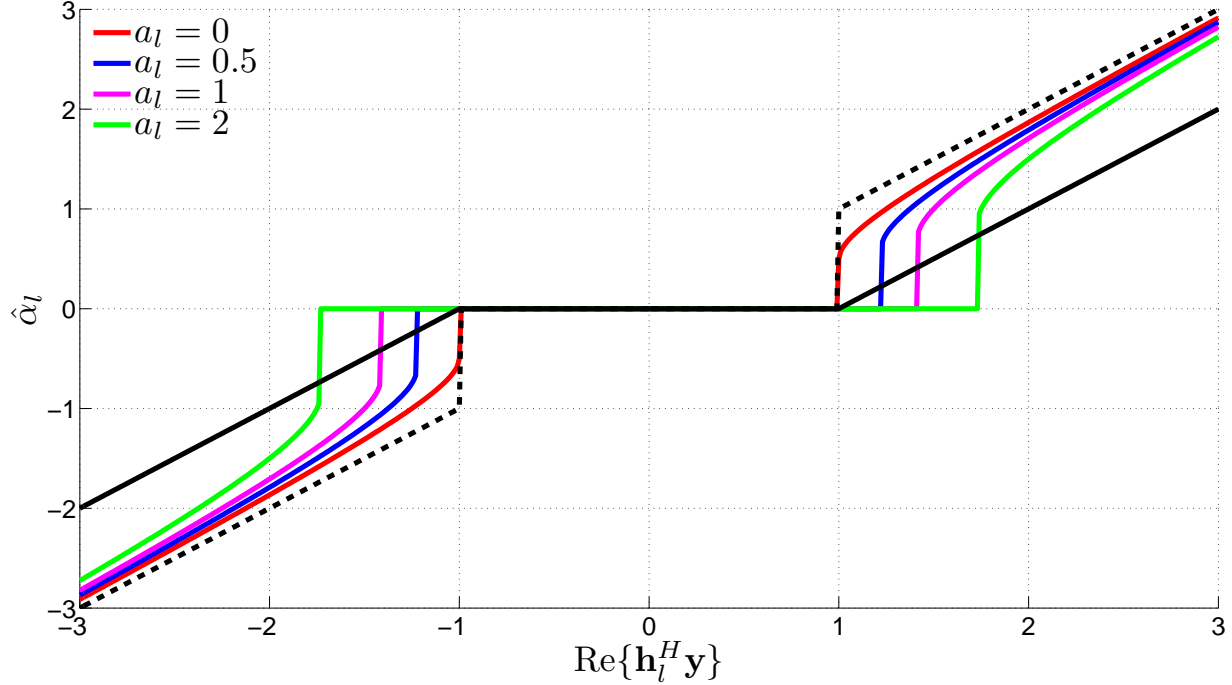


Fig. 4. Three-layer hierarchical prior for the complex system model with small  $b$  ( $b = 10^{-6}$ ): Restriction to  $\text{Im}\{\mathbf{h}_l^H \mathbf{y}\} = 0$  of the resulting MAP estimation rule (2) with  $a_l$  as a parameter in the case when  $\mathbf{H}$  is orthonormal. The black dashed line indicates the hard-threshold rule and the black solid line the soft-threshold rule (11).

diffuse prior over  $\boldsymbol{\eta}$ . This can be achieved by selecting the entries in  $\mathbf{b}$  to be small; practically, we set  $b_l = 10^{-6}$ ,  $l = 1, \dots, L$ . For small  $b_l$  the prior (13) can be approximated as

$$p(\gamma_l; \epsilon, a_l, b_l) \approx \frac{b_l^{a_l} \Gamma(\epsilon + a_l)}{\Gamma(\epsilon) \Gamma(a_l)} \gamma_l^{-(a_l+1)}. \quad (16)$$

If in addition we select  $\epsilon = 0$  we obtain the improper prior for  $\gamma_l$

$$p(\gamma_l; a_l) \propto \gamma_l^{-(a_l+1)}. \quad (17)$$

The prior  $p(\alpha_l; a_l)$  obtained by marginalizing  $p(\alpha_l | \gamma_l) p(\gamma_l; a_l)$  over  $\gamma_l$  is also improper in this case:

$$p(\alpha_l; a_l) \propto |\alpha_l|^{-2(a_l+\rho)}. \quad (18)$$

The prior (18) leads to a weighted log-sum penalty term  $Q(\boldsymbol{\alpha}; \mathbf{a}) = 2 \sum_{l=1}^L (a_l + \rho) \log |\alpha_l|$  parametrized by  $\mathbf{a}$  in the MAP objective function. Observe that selecting  $\mathbf{a} = \mathbf{0}$  in (18) the log-sum penalty term is automatically obtained. Such form of penalty appears in the ARD formulation of the G-IGa prior model [12], [21], as well as in the re-weighted  $\ell_1$  optimization [8].

The dependency of (18) on  $a_l$  gives some extra degree of freedom to further adjust the sparsity property of this prior. To demonstrate this, let us again consider the special case of an orthogonal measurement matrix  $\mathbf{H}$ . In Fig. 4 we depict the corresponding MAP estimation rules for  $\alpha_l$  with penalty term  $Q(\alpha_l; a_l) = 2(a_l + \rho) \log |\alpha_l|$ . Observe that increasing the value of  $a_l$  also increases the values of the effective threshold, thus resulting in sparser solutions of  $\boldsymbol{\alpha}$ .

### III. RELATED APPROACHES AND METHODS

In this section we establish the relationship between the sparse Bayesian modeling approach with hierarchical priors developed in Sec. II and other state-of-the-art sparse estimation techniques proposed in the literature.

The iterative re-weighted  $\ell_1$  minimization method studied by [8], [10], [21] solves the weighted optimization problem for the real system model ( $\rho = 1/2$ ) in (2) with penalty term

$$Q(\boldsymbol{\alpha}; \boldsymbol{\beta}) = \sum_{l=1}^L \beta_l |\alpha_l|, \quad (19)$$

where  $\beta_l$ ,  $l = 1, \dots, L$ , are some fixed weights. In [8] it is proposed to update the weights as

$$\beta_l = (|\hat{\alpha}_l| + \varsigma)^{-1}, \quad (20)$$

where  $\varsigma$  is some small constant and  $\hat{\alpha}_l$  is the current estimate of  $\alpha_l$ ; such an algorithm leads to a sequence of re-weighted  $\ell_1$  minimization problems.

We show that our proposed G-Ga prior model also implements the same objective function, albeit for real as well as complex system models. Indeed, the MAP estimate of  $\boldsymbol{\alpha}$  computed using the G-Ga hierachal prior model with the setting  $\epsilon = \rho + 1/2$  yields the penalty term

$$Q(\boldsymbol{\alpha}; \boldsymbol{\eta}) = 2 \sum_{l=1}^L \sqrt{\rho \eta_l} |\alpha_l|. \quad (21)$$

Hence, (21) is equivalent to (19) with the weighting factors  $\beta_l = 2\sqrt{\rho \eta_l}$ ,  $l = 1, \dots, L$ . Quite naturally this relationship can be exploited by selecting the hyperparameters  $\eta_l = 1/(4\rho(|\hat{\alpha}_l| + \varsigma)^2)$  as proposed in [8]. Moreover, in contrast to [8] and as already mentioned in Sec. II, the Bayesian hierarchical approach is not constrained to the  $\ell_1$ -type of penalty term obtained with  $\epsilon = \rho + 1/2$ , but can be used for arbitrary values of  $\epsilon$ , leading to the general re-weighted constrained optimization problem by updating  $\eta_l$  in (10). We will demonstrate that due to the strong sparsity-inducing nature of the prior (7) for  $\epsilon < \rho + 1/2$ , (10) leads to a sparser estimate as compared to that obtained using (21).

Similarly to the G-Ga prior model, the two-layer G-IGa prior model proposed in [12] also requires specifying the hyperprior parameters. In [12] the variance  $\gamma_l$  follows an inverse gamma distribution. The corresponding marginal distribution of  $\alpha_l$  can be shown to follow a Student-t distribution. This result can be easily generalized for complex variables, leading to the prior for  $\alpha_l$

$$p(\alpha_l; a_l, b_l) = \left(\frac{\rho}{\pi}\right)^{\rho} \frac{b_l^{a_l} \Gamma(a_l + \rho)}{\Gamma(a_l)} (b_l + \rho|\alpha_l|^2)^{-(a_l + \rho)}. \quad (22)$$

Setting  $a_l$  and  $b_l$  to zero leads to a special case of non-informative hyperpriors and ARD, with an improper prior  $p(\alpha) \propto \prod_{l=1}^L |\alpha_l|^{-2\rho}$  that leads to the log-sum penalty term  $Q(\alpha) = 2\rho \sum_{l=1}^L \log |\alpha_l|$ . We should also add that the  $\ell_1$  re-weighting scheme in [8] has also been motivated using the log-sum penalty term (see [8] for more details). Moreover, it has been demonstrated [10], [21] that the ARD approach to SBL based on the G-IGa prior model can also be interpreted as a series of re-weighted  $\ell_1$  minimization problems; the computation of the weighting factors, however, differs from that used in [8].

Similarly, in [16] the author also suggests to make use of Jeffreys' prior for the variance  $\gamma_l$  in the G-E prior model. It can be shown that this choice of hyperprior in fact again leads to the same improper ARD prior  $p(\alpha_l) \propto |\alpha_l|^{-2\rho}$ . Hence, the G-IGa model proposed by Tipping in [12] and the G-E model proposed by Figueiredo in [16] are equivalent when the hyperpriors are chosen to be non-informative. Note that since the G-Ga prior model endorses the G-E model as a special case, the same is true when  $\epsilon = \eta_l = 0$ ,  $l = 1, \dots, L$ , in (7). Furthermore, for the three-layer prior model it is easily seen that letting  $a_l = b_l = \epsilon = 0$  in (13) also entails the non-informative Jeffreys' prior for  $\gamma_l$ . Thus, the equivalent marginalized prior  $p(\alpha_l)$  coincides with that obtained in [12] and [16] when non-informative hyperpriors are assumed. In other words, when second or third layer priors are chosen to be non-informative, an instance of ARD is obtained regardless of the hierachal prior model used.

While two-layer models in general require specifying the regularization parameters, three-layer prior models effectively lead to an alternative automatic procedure for selecting the parameters  $\eta_l$ . The three-layer structure has been implicitly exploited in [5] for sparse variational Bayesian extension of the SAGE algorithm for parameter estimation in sparse wireless channels and explicitly in [7] for hierarchical adaptive LASSO. In [5] the authors exploit the two-layer prior structure, where the first layer is the  $\ell_1$  prior, i.e.,  $p(\alpha|\tilde{\eta}) \propto \prod_{l=1}^L \exp(-2\tilde{\eta}_l|\alpha_l|)$  and the second layer is the gamma hyperprior  $p(\tilde{\eta}) = \prod_{l=1}^L \text{Ga}(\tilde{\eta}_l|a_l, b_l)$ . Obviously, the prior  $p(\alpha|\tilde{\eta})$  can be constructed via the G-Ga model as we showed in Sec. II-A with  $\tilde{\eta}_l = \sqrt{\eta_l}$ ; thus, the two-layer  $\ell_1$ -gamma prior model used in [5] is equivalent to the three-layer structure discussed in Sec. II-B with the selected hyper-hyperprior  $p(\eta) = \prod_{l=1}^L \text{Ga}(\sqrt{\eta_l}|a_l, b_l)$ .

Thus,  $\tilde{\eta}_l = \sqrt{\eta_l}$  following a generalized gamma distribution [22]. The resulting update expressions for  $\tilde{\eta}_l$  can then be computed as [5], [7]

$$\tilde{\eta}_l = \frac{a_l + \rho^{-1}}{b_l + \rho^{-1}|\hat{\alpha}_l|}. \quad (23)$$

Notice the similarity between the update expression (23) and the one proposed in [8] for the weights  $\beta_l$  in (19). Let us stress that although the authors in [7] discuss the three-layer structure, they do not exploit the hierarchy for constructing the inference algorithm; instead, the first two layers are combined together to give the Laplace prior. This leads to the desired LASSO-type objective function for estimating  $\alpha$  and makes their approach numerically equivalent to that proposed in [5]. Nonetheless, despite formal similarities between the update expressions for the  $\ell_1$  weighting parameters obtained with the three-layer hierarchical prior and those proposed in [8], a substantial difference between these schemes lies in the order in which the parameters are updated. Specifically, in [8] the weights are updated once a single weighted  $\ell_1$  optimization problem has been solved with fixed weights  $\eta_l$ ,  $l = 1, \dots, L$ ; similarly, the ARD approach estimates the corresponding weighting parameters once the vector  $\alpha$  that optimizes the ARD objective function are computed [21]. In contrast, in [5] and [7] the update expressions for the weights of the weighted  $\ell_1$  optimization are evaluated concurrently with the update expressions for the model parameter vector  $\alpha$ ; in other words, a weight  $\eta_l$  is updated each time the corresponding parameter  $\alpha_l$  is updated.

#### IV. VARIATIONAL MESSAGE PASSING

In this section we present a variational message passing (VMP) algorithm for estimating  $\alpha$  given the observation  $\mathbf{y}$ . First, we derive the VMP inference expressions for the SBL problem with the two- and the three-layer prior models. Then, a procedure for removing a basis function from the measurement matrix  $\mathbf{H}$  is described.

##### A. The VMP algorithm

Let  $\Phi = \{\alpha, \gamma, \eta, \lambda\}$  be the set of unknown parameters to be estimated and let  $p(\mathbf{y}, \Phi)$  be the joint pdf specified in (4). The factor graph [23] that encodes the factorization of  $p(\mathbf{y}, \Phi)$  in (4) is shown in Fig. 5. Consider an auxiliary pdf  $q(\Phi)$  for the unknown parameters that factorizes according to  $q(\Phi) = q(\alpha)q(\gamma)q(\eta)q(\lambda)$ . The VMP algorithm is an iterative scheme that attempts to compute the auxiliary pdf  $q(\Phi)$  by minimizing the Kullback-Leibler (KL) divergence  $\text{KL}(q(\Phi) \parallel p(\Phi|\mathbf{y}))$ . In the following we summarize its key steps; the reader is referred to [24] for more information on VMP.

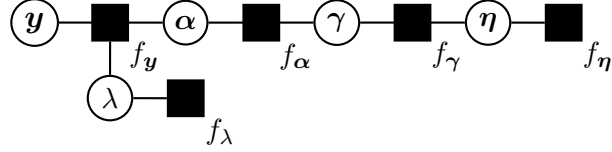


Fig. 5. A factor graph [23] that represents the joint pdf (4). In this figure  $f_y \equiv p(\mathbf{y}|\boldsymbol{\alpha}, \lambda)$ ,  $f_\alpha \equiv p(\boldsymbol{\alpha}|\boldsymbol{\gamma})$ ,  $f_\gamma \equiv p(\boldsymbol{\gamma})$ ,  $f_\eta \equiv p(\boldsymbol{\eta})$ , and  $f_\lambda \equiv p(\lambda)$ .

From [24] the auxiliary function  $q(\phi_i)$ ,  $\phi_i \in \boldsymbol{\phi}$  is updated as the product of incoming messages from the neighboring factor nodes  $f_n$  to the variable node  $\phi_i$ :

$$q(\phi_i) \propto \prod_{f_n \in \mathcal{N}_{\phi_i}} m_{f_n \rightarrow \phi_i}. \quad (24)$$

In (24)  $\mathcal{N}_{\phi_i}$  is the set of factor nodes neighboring the variable node  $\phi_i$  and  $m_{f_n \rightarrow \phi_i}$  denotes the message from factor node  $f_n$  to variable node  $\phi_i$ . This message is computed as

$$m_{f_n \rightarrow \phi_i} = \exp \left( \langle \ln f_n \rangle_{\prod_j q(\phi_j), \phi_j \in \mathcal{N}_{f_n} \setminus \{\phi_i\}} \right), \quad (25)$$

where  $\mathcal{N}_{f_n}$  is the set of variable nodes neighboring the factor node  $f_n$ . After an initialization procedure, the individual factors of  $q(\boldsymbol{\Phi})$  are then updated iteratively in a round-robin fashion using (24) and (25).

In the following we derive two versions of the VMP algorithm: one applied to the two-layer G-Ga prior model (referred to as VMP-2L), and another one applied to the three-layer G-Ga-Ga model (VMP-3L). The messages corresponding to VMP-2L are easily obtained as a special case of the messages computed for VMP-3L by assuming  $q(\eta_l) = \delta(\eta_l - \hat{\eta}_l)$ , where  $\delta(\cdot)$  is a Dirac delta function and  $\hat{\eta}_l$  is some fixed number. We compute the messages for both real-valued ( $\rho = 1/2$ ) and complex-valued ( $\rho = 1$ ) signal models (1).

1) *Update of  $q(\boldsymbol{\alpha})$ :* According to (24) the computation of  $q(\boldsymbol{\alpha})$  requires evaluating the product of messages  $m_{p_{\mathbf{y} \rightarrow \boldsymbol{\alpha}}}$  and  $m_{p_{\boldsymbol{\alpha} \rightarrow \boldsymbol{\alpha}}}$ . These are obtained as

$$\begin{aligned} m_{p_{\mathbf{y} \rightarrow \boldsymbol{\alpha}}} &= \exp(\langle \ln p(\mathbf{y}|\boldsymbol{\alpha}, \lambda) \rangle_{q(\lambda)}) \\ &\propto \exp(-\rho \langle \lambda \rangle_{q(\lambda)} \|\mathbf{y} - \mathbf{H}\boldsymbol{\alpha}\|_2^2), \end{aligned} \quad (26)$$

$$\begin{aligned} m_{p_{\boldsymbol{\alpha} \rightarrow \boldsymbol{\alpha}}} &= \exp(\langle \ln p(\boldsymbol{\alpha}|\boldsymbol{\gamma}) \rangle_{q(\boldsymbol{\gamma})}) \\ &\propto \exp(-\rho \boldsymbol{\alpha}^H \mathbf{V}(\boldsymbol{\gamma}) \boldsymbol{\alpha}), \end{aligned} \quad (27)$$

where we define  $\mathbf{V}(\boldsymbol{\gamma}) = \text{diag}\{\langle \gamma_1^{-1} \rangle_{q(\boldsymbol{\gamma})}, \dots, \langle \gamma_L^{-1} \rangle_{q(\boldsymbol{\gamma})}\}$ . Multiplying (26) and (27) yields the Gaussian auxiliary pdf  $q(\boldsymbol{\alpha}) = \text{CN}(\boldsymbol{\alpha} | \hat{\boldsymbol{\alpha}}, \hat{\boldsymbol{\Sigma}}_{\boldsymbol{\alpha}})$  when  $\rho = 1$  and  $q(\boldsymbol{\alpha}) = \mathcal{N}(\boldsymbol{\alpha} | \hat{\boldsymbol{\alpha}}, \hat{\boldsymbol{\Sigma}}_{\boldsymbol{\alpha}})$  when  $\rho = 1/2$  with corresponding mean and covariance given by

$$\hat{\boldsymbol{\Sigma}}_{\boldsymbol{\alpha}} = (\langle \lambda \rangle_{q(\lambda)} \mathbf{H}^H \mathbf{H} + \mathbf{V}(\boldsymbol{\gamma}))^{-1}, \quad (28)$$

$$\hat{\boldsymbol{\alpha}} = \langle \boldsymbol{\alpha} \rangle_{q(\boldsymbol{\alpha})} = \langle \lambda \rangle_{q(\lambda)} \hat{\boldsymbol{\Sigma}}_{\boldsymbol{\alpha}} \mathbf{H}^H \mathbf{y}. \quad (29)$$

2) *Update of  $q(\boldsymbol{\gamma})$ :* The computation of  $q(\boldsymbol{\gamma})$  requires evaluating the messages  $m_{p_{\boldsymbol{\alpha}} \rightarrow \boldsymbol{\gamma}}$  and  $m_{p_{\boldsymbol{\gamma}} \rightarrow \boldsymbol{\gamma}}$ :

$$\begin{aligned} m_{p_{\boldsymbol{\alpha}} \rightarrow \boldsymbol{\gamma}} &= \exp(\langle \ln p(\boldsymbol{\alpha} | \boldsymbol{\gamma}) \rangle_{q(\boldsymbol{\alpha})}) \\ &\propto \prod_{l=1}^L \gamma_l^{-\rho} \exp(-\rho \gamma_l^{-1} \langle |\alpha_l|^2 \rangle_{q(\boldsymbol{\alpha})}), \end{aligned} \quad (30)$$

$$m_{p_{\boldsymbol{\gamma}} \rightarrow \boldsymbol{\gamma}} \propto \prod_{l=1}^L \gamma_l^{\epsilon-1} \exp(-\gamma_l \langle \eta_l \rangle_{q(\boldsymbol{\eta})}). \quad (31)$$

Notice that  $\langle |\alpha_l|^2 \rangle_{q(\boldsymbol{\alpha})}$  in (30) is the  $l$ th diagonal element of  $\langle \boldsymbol{\alpha} \boldsymbol{\alpha}^H \rangle_{q(\boldsymbol{\alpha})} = \hat{\boldsymbol{\Sigma}}_{\boldsymbol{\alpha}} + \hat{\boldsymbol{\alpha}} \hat{\boldsymbol{\alpha}}^H$ . Multiplying (30) and (31) yields

$$q(\boldsymbol{\gamma}) \propto \prod_{l=1}^L \gamma_l^{\epsilon-\rho-1} \exp(-\gamma_l^{-1} \rho \langle |\alpha_l|^2 \rangle_{q(\boldsymbol{\alpha})} - \gamma_l \langle \eta_l \rangle_{q(\boldsymbol{\eta})}). \quad (32)$$

The right-hand side expression in (32) is recognized as the product of Generalized Inverse Gaussian (GIG) pdfs [25], i.e.,  $q(\boldsymbol{\gamma}) = \prod_{l=1}^L q(\gamma_l; p, u_l, v_l)$  where  $q(\gamma_l; p, u_l, v_l) = \frac{(u_l/v_l)^{\frac{p}{2}}}{2K_p(\sqrt{u_l v_l})} \gamma_l^{p-1} \exp\left(-\frac{u_l}{2}\gamma_l - \frac{v_l}{2}\gamma_l^{-1}\right)$  with order  $p = \epsilon - \rho$  and parameters  $u_l = 2\langle \eta_l \rangle_{q(\boldsymbol{\eta})}$  and  $v_l = 2\rho \langle |\alpha_l|^2 \rangle_{q(\boldsymbol{\alpha})}$ .

Observe that the computation of  $\mathbf{V}(\boldsymbol{\gamma})$  in (28) requires evaluating  $\langle \gamma_l^{-1} \rangle_{q(\boldsymbol{\gamma})}$  for all  $l = 1, \dots, L$ . Luckily, the moments of the GIG distribution are given in closed form for any  $n \in \mathbb{R}$  [25]:

$$\langle \gamma_l^n \rangle_{q(\boldsymbol{\gamma})} = \left( \frac{\rho \langle |\alpha_l|^2 \rangle_{q(\boldsymbol{\alpha})}}{\langle \eta_l \rangle_{q(\boldsymbol{\eta})}} \right)^{\frac{n}{2}} \frac{K_{p+n} \left( 2\sqrt{\rho \langle \eta_l \rangle_{q(\boldsymbol{\eta})} \langle |\alpha_l|^2 \rangle_{q(\boldsymbol{\alpha})}} \right)}{K_p \left( 2\sqrt{\rho \langle \eta_l \rangle_{q(\boldsymbol{\eta})} \langle |\alpha_l|^2 \rangle_{q(\boldsymbol{\alpha})}} \right)}. \quad (33)$$

In the special case of  $\ell_1$ -norm priors, i.e., when  $p = \epsilon - \rho = 1/2$ , using the identity  $K_{\nu}(\cdot) = K_{-\nu}(\cdot)$  [19], (33) simplifies to

$$\langle \gamma_l^{-1} \rangle_{q(\boldsymbol{\gamma})} = \left( \frac{\langle \eta_l \rangle_{q(\boldsymbol{\eta})}}{\rho \langle |\alpha_l|^2 \rangle_{q(\boldsymbol{\alpha})}} \right)^{\frac{1}{2}}. \quad (34)$$

3) *Update of  $q(\boldsymbol{\eta})$ :* The update of  $q(\boldsymbol{\eta})$  is the product of messages  $m_{p_{\boldsymbol{\eta}} \rightarrow \boldsymbol{\eta}}$  and  $m_{p_{\boldsymbol{\gamma}} \rightarrow \boldsymbol{\eta}}$ :

$$q(\boldsymbol{\eta}) \propto \prod_{l=1}^L \eta_l^{\epsilon+a_l-1} \exp \left( -(\langle \gamma_l \rangle_{q(\boldsymbol{\gamma})} + b_l) \eta_l \right), \quad (35)$$

which is identified as a gamma pdf. The first moment of  $\eta_l$  used in (33) is easily computed as

$$\langle \eta_l \rangle_{q(\boldsymbol{\eta})} = \frac{\epsilon + a_l}{\langle \gamma_l \rangle_{q(\boldsymbol{\gamma})} + b_l}. \quad (36)$$

Naturally,  $q(\boldsymbol{\eta})$  is only computed for VMP-3L.

4) *Update of  $q(\lambda)$ :* The update of  $q(\lambda)$  can be shown to be  $q(\lambda) = \text{Ga}(\lambda | \rho M + c, \rho \langle \|\mathbf{y} - \mathbf{H}\boldsymbol{\alpha}\|_2^2 \rangle_{q(\boldsymbol{\alpha})} + d)$ . The first moment of  $\lambda$  used in (28) and (29) is therefore computed as

$$\langle \lambda \rangle_{q(\lambda)} = \frac{\rho M + c}{\rho \langle \|\mathbf{y} - \mathbf{H}\boldsymbol{\alpha}\|_2^2 \rangle_{q(\boldsymbol{\alpha})} + d}. \quad (37)$$

### B. Pruning a basis function

When the estimation algorithm produces a sparse parameter vector  $\hat{\boldsymbol{\alpha}}$  with  $\hat{K}$  non-zero components, the remaining  $L - \hat{K}$  basis function in the measurement matrix  $\mathbf{H}$  can be removed from the model. This basis function pruning drastically lowers the computational complexity of the VMP algorithm. Specifically, it reduces the computational complexity of the inversion of the covariance matrix in (28) from  $O(L^3)$  to  $O(\hat{K}^3)$ .

A closer inspection of (28) reveals that the parameters  $\langle \gamma_l^{-1} \rangle_{q(\boldsymbol{\gamma})}$  are in fact classical regularization terms for estimating the weights  $\boldsymbol{\alpha}$ . Quite naturally, the larger the value of  $\langle \gamma_l^{-1} \rangle_{q(\boldsymbol{\gamma})}$ , i.e., the larger the regularization for the  $l$ th basis function  $\mathbf{h}_l$ , the smaller the estimate of the corresponding  $\alpha_l$ . Thus, it makes sense to remove  $\mathbf{h}_l$  in  $\mathbf{H}$  when  $\langle \gamma_l^{-1} \rangle_{q(\boldsymbol{\gamma})}$  exceeds a certain large threshold. The same method was used in [12] for the G-IGa prior model to obtain a sparse solution.

## V. NUMERICAL RESULTS

We perform Monte Carlo simulations to evaluate the performance of the two versions of the derived VMP algorithm in Sec. IV. A complex-valued signal model (1) is considered in all experiments, where for each Monte Carlo run a random  $M \times L$  matrix  $\mathbf{H}$ , a  $K$ -sparse vector  $\boldsymbol{\alpha}$ , and a random perturbation vector  $\mathbf{w}$  are generated. In order to test the methods on a realistic benchmark we use a random dictionary  $\mathbf{H}$  whose entries are independent and identically distributed (iid) zero-mean complex symmetric Gaussian random variables with unit variance. The indices of the  $K$  non-zero components of  $\boldsymbol{\alpha}$  are uniformly drawn from the set  $\{1, 2, \dots, L\}$ . The  $K$  non-zero components of  $\boldsymbol{\alpha}$  are iid and drawn from a zero-mean

Legend	Model	Parameters
VMP-2L( $\epsilon = 3/2$ )	G-Ga	$\epsilon = 3/2$
VMP-2L( $\epsilon = 0$ )	G-Ga	$\epsilon = 0$
VMP-3L( $\epsilon = 3/2$ )	G-Ga-Ga	$\epsilon = 3/2, \mathbf{a} = \mathbf{1}, \mathbf{b} = 10^{-6}\mathbf{1}$
VMP-3L( $\epsilon = 0$ )	G-Ga-Ga	$\epsilon = 0, \mathbf{a} = \mathbf{1}, \mathbf{b} = 10^{-6}\mathbf{1}$

TABLE I  
THE SELECTED PARAMETERS FOR THE PROPOSED PRIOR MODELS PRESENTED IN SEC. II. HERE,  $\mathbf{1} := [1, \dots, 1]^T$ .

complex circular symmetric Gaussian distribution with unit variance. All reported curves are computed based on a total of 200 Monte Carlo runs.

Table I summarizes the choice of the free parameters for the G-Ga and G-Ga-Ga prior models discussed in Sec. II. As indicated in the table, the selected value of  $\epsilon$  used in the different versions of the VMP algorithm is appended to their acronyms.

To initialize the VMP algorithm we set  $\langle \lambda \rangle_{q(\lambda)}$  equal to  $(\text{Var}\{\mathbf{y}\})^{-1}$  and  $\langle \gamma_l^{-1} \rangle_{q(\gamma)}$  equal to the inverse number of columns  $L$ . Furthermore, we let  $c = d = 0$  in (37), which corresponds to a non-informative prior for  $\lambda$ . Once the initialization is completed, the algorithm sequentially updates the auxiliary pdfs  $q(\boldsymbol{\alpha})$ ,  $q(\boldsymbol{\gamma})$ ,  $q(\lambda)$ , and  $q(\boldsymbol{\eta})$  until convergence is achieved. As stated in Sec. IV,  $q(\boldsymbol{\eta})$  is only updated for VMP-3L, whereas for VMP-2L the entries in  $\boldsymbol{\eta}$  are free parameters that must be determined. Therefore, we propose to use the re-weighting scheme of [8] to update  $\eta_l$  once the VMP-2L algorithm has converged and a solution  $\hat{\alpha}_l$  is produced. The parameters  $\eta_l$ ,  $l = 1, \dots, L$ , are then updated based on the corresponding estimates  $\hat{\alpha}_l$  and the VMP-2L algorithm is iterated once more with the updated parameters. Specifically,  $\eta_l$  is updated as [8]

$$\eta_l = (|\hat{\alpha}_l| + \varsigma)^{-2} \quad (38)$$

with the parameter  $\varsigma$  set to  $\varsigma = 10^{-3}$ . Empirically we have observed that only a few (roughly 3 – 4) re-weighting updates are needed. Initially, we choose  $\boldsymbol{\eta} = [1, \dots, 1]^T$  the first time the VMP-2L algorithm solves the optimization problem.

In the sequel we perform the following investigations: first, the performance of the VMP-2L and VMP-3L is analyzed; then, the VMP algorithm is compared with several state-of-the-art sparse estimation schemes. The performance of the compared algorithms is evaluated based on the mean-squared error (MSE) of  $\hat{\boldsymbol{\alpha}}$  and the number of non-zero elements  $\hat{K}$  in  $\hat{\boldsymbol{\alpha}}$ . Note that the estimate  $\hat{\alpha}_l$  is set to zero when  $\langle \gamma_l^{-1} \rangle_{q(\gamma)}$  exceeds a fixed threshold set at  $10^6$ .

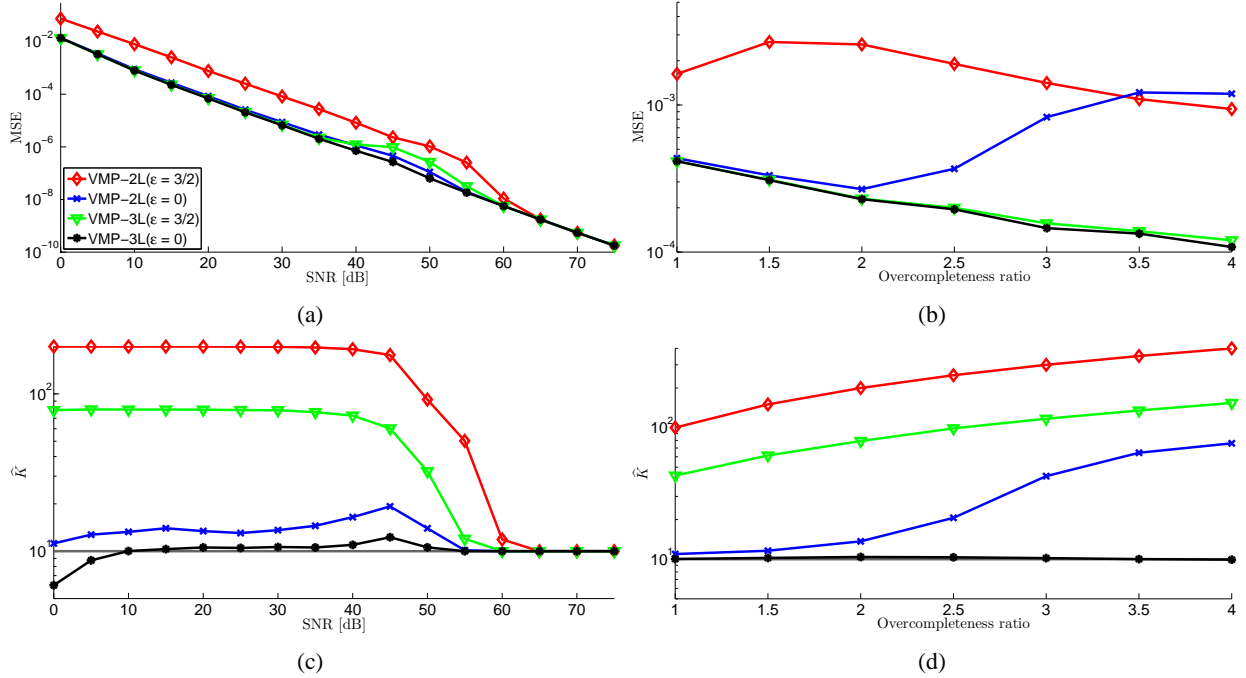


Fig. 6. Performance of the VMP algorithm: (a,b) MSE versus (a) SNR and (b) overcompleteness ratio  $L/M$  with  $M = 100$ . (c,d) Estimated number of non-zero components  $\hat{K}$  versus (c) SNR and (d) overcompleteness ratio  $L/M$  ( $M=100$ ) at 15 dB SNR. The gray horizontal line indicates the true number of non-zero components in  $\alpha$ .

### A. Performance of the VMP algorithm

Here we evaluate the performance of the VMP algorithm versus (i) the SNR per received signal component and (ii) the overcompleteness ratio  $L/M$ . The results illustrate the sensitivity of the algorithm to measurement noise and its performance in classical compressive sampling test setting, where the number of basis functions  $L$  exceeds the number of measurements samples  $M$ . In these investigations the true number of non-zero components in  $\alpha$  is set to  $K = 10$ .

In Figs. 6(a) and 6(c) the performance of the algorithm is evaluated versus the SNR with  $M = 100$  and  $L = 200$ , which yields an overcompleteness ratio of  $L/M = 2$ . Notice that in a very high SNR regime, i.e., when the observation is practically noise free, the performance of the compared schemes is almost indistinguishable. However, when the noise cannot be neglected, VMP-3L( $\epsilon = 0$ ) clearly outperforms the other three schemes in terms of the estimate  $\hat{K}$ , followed closely by VMP-2L( $\epsilon = 0$ ); VMP-2L( $\epsilon = 3/2$ ) clearly performs worse than the other schemes both in terms of the achieved sparseness and MSE. Observe that when  $\epsilon = 3/2$ , which is equivalent to the  $\ell_1$ -norm parameter constraint, both G-Ga and G-Ga-Ga models induce a heavily overestimation of  $K$ ; in contrast, setting  $\epsilon = 0$  leads to much sparser solutions. Also, notice that for a fixed  $\epsilon$ , the G-Ga-Ga model generally leads to an estimator that produces sparser

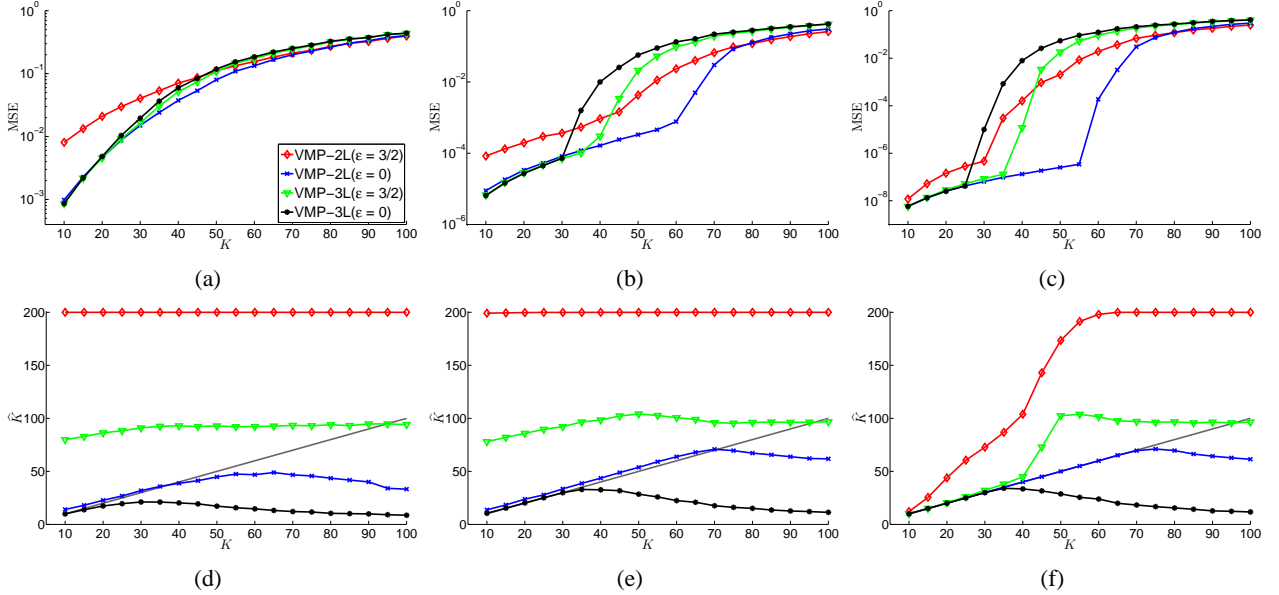


Fig. 7. Performance of the VMP algorithm: (a)-(c) MSE performance and (d)-(f) estimated number of non-zero components  $\hat{K}$  versus the true number of non-zero components  $K$ . The SNR is set to 10 dB in (a) and (d), 30 dB in (b) and (e), and 60 dB in (c) and (f).

results as compared to that of the G-Ga model.

In Figs. 6(b) and 6(d) the performance of the algorithm is compared as a function of the overcompleteness ratio  $L/M$  for an SNR level fixed at 15 dB. Here again VMP-3L( $\epsilon = 0$ ) is a clear winner. We also notice that for a fixed  $\epsilon$  the G-Ga-Ga model induces better performance over the G-Ga model, and the case  $\epsilon = 0$  outperforms the schemes realizing the  $\ell_1$ -norm parameter constraints with  $\epsilon = 3/2$ .

Next we evaluate the performance of the schemes as a function of the number of non-zero components  $K$  in  $\alpha$ . To this end we set  $M = 100$ ,  $L = 200$  and vary  $K$  from 10 to  $M$ . The MSE and the estimate  $\hat{K}$  are compared for SNR fixed at 10 dB, 30 dB, and 60 dB. The corresponding results are shown in Fig. 7. In low SNR regime ( $\sim 10$  dB) VMP-2L( $\epsilon = 0$ ), VMP-3L( $\epsilon = 3/2$ ), and VMP-3L( $\epsilon = 0$ ) exhibit an almost identical MSE performance, with VMP-2L( $\epsilon = 3/2$ ) performing worse only for low  $K$  values. However,  $\hat{K}$  does vary for these schemes. For  $\epsilon = 3/2$  the estimate  $\hat{K}$  is almost independent of the true number of non-zero components  $K$ . However, when  $\epsilon = 0$ , VMP-3L( $\epsilon = 0$ ) underestimates  $K$ , performing best only if  $K < 20$ ; in contrast VMP-2L( $\epsilon = 0$ ) exhibits acceptable performance for  $K < 40$ . As the SNR increases, the performance of all schemes improves, yet the MSE curves begin to exhibit an interesting thresholding effect, which gives the highest  $K$  value for which the algorithm is still able to recover the true number of non-zero components. Here, VMP-2L( $\epsilon = 0$ ) performs the best, exhibiting the thresholding behavior at  $K \approx 60$  or even  $K \approx 70$  as the SNR grows to 60 dB. It

is followed by VMP-3L( $\epsilon = 0$ ), exhibiting the thresholding effect already at  $K \approx 30$  for both 30 dB and 60 dB SNR. However, the performance of both schemes with  $\epsilon = 0$  significantly degrades when  $K$  increases beyond the corresponding sparsity threshold levels, i.e., when the signal becomes less sparse. Specifically, the number of non-zero components in  $\alpha$  is underestimated, leading to an abrupt increase in the MSE of the estimates. The VMP schemes with  $\epsilon = 3/2$  become effective only when the SNR level becomes very high, with VMP-3L( $\epsilon = 3/2$ ) inducing superior performance than VMP-2L( $\epsilon = 3/2$ ).

In what follows we compare the performance of VMP-2L( $\epsilon = 0$ ) and VMP-3L( $\epsilon = 0$ ) with several other sparse estimation algorithms.

### B. Comparison with Existing Sparse Methods

In the following, we compare VMP-2L( $\epsilon = 0$ ) and VMP-3L( $\epsilon = 0$ ) to the ARD formulation of the RVM [12], [13], the *sparse reconstruction by separable approximation* (SpaRSA) algorithm [26],<sup>7</sup> and a re-weighted version of SpaRSA. The SpaRSA algorithm is a proximal gradient method for solving the LASSO cost function. We can easily extend the framework of [26] to solve the weighted LASSO cost function:

$$\hat{\mathbf{z}} = \underset{\mathbf{z} \in \mathbb{C}^L}{\operatorname{argmin}} \left\{ \frac{1}{2} \|\mathbf{y} - \mathbf{H}\mathbf{B}^{-1}\mathbf{z}\|_2^2 + \kappa \|\mathbf{z}\|_1 \right\}, \quad (39)$$

where  $\alpha = \mathbf{B}^{-1}\mathbf{z}$  and  $\mathbf{B} \triangleq \operatorname{diag}\{\beta\}$ . The components of  $\beta \triangleq [\beta_1, \dots, \beta_L]^T$  are updated according to (20) with  $\varsigma = 10^{-3}$  a total of 3 times. Further in the text we will refer to this algorithm as Reweighted SpaRSA. Note that the choice of  $\kappa$  has a crucial impact on the performance of the resulting inference. For large  $\kappa$  the algorithm produces very sparse estimates; however, the MSE performance in this case might significantly degrade. In our implementation of this estimation scheme we select  $\kappa = 0.2$  for SpaRSA and  $\kappa = 0.05$  for Reweighted SpaRSA. The latter values were empirically found to balance well the achieved signal sparsity with the MSE. As already mentioned, VMP-3L, in contrast, provides the necessary mechanism to set this regularization parameter automatically.

In Fig. 8 the performance of the compared schemes is depicted for  $K = 10$ . In Figs. 8(a), 8(c) the dependency of the estimates' MSE on the SNR for the overcompleteness ratio  $L/M = 2$  with  $M = 100$  is visualized. Observe that VMP-2L( $\epsilon = 0$ ) and VMP-3L( $\epsilon = 0$ ) achieve lower MSE in the SNR range up to 60 dB as compared to the other schemes. Furthermore, in this SNR range they also produce sparser estimates. However, Reweighted SpaRSA "catches" the VMP curves already at 30 dB, slightly

<sup>7</sup>The software is available on-line at <http://www.lx.it.pt/~mtf/SpaRSA/>

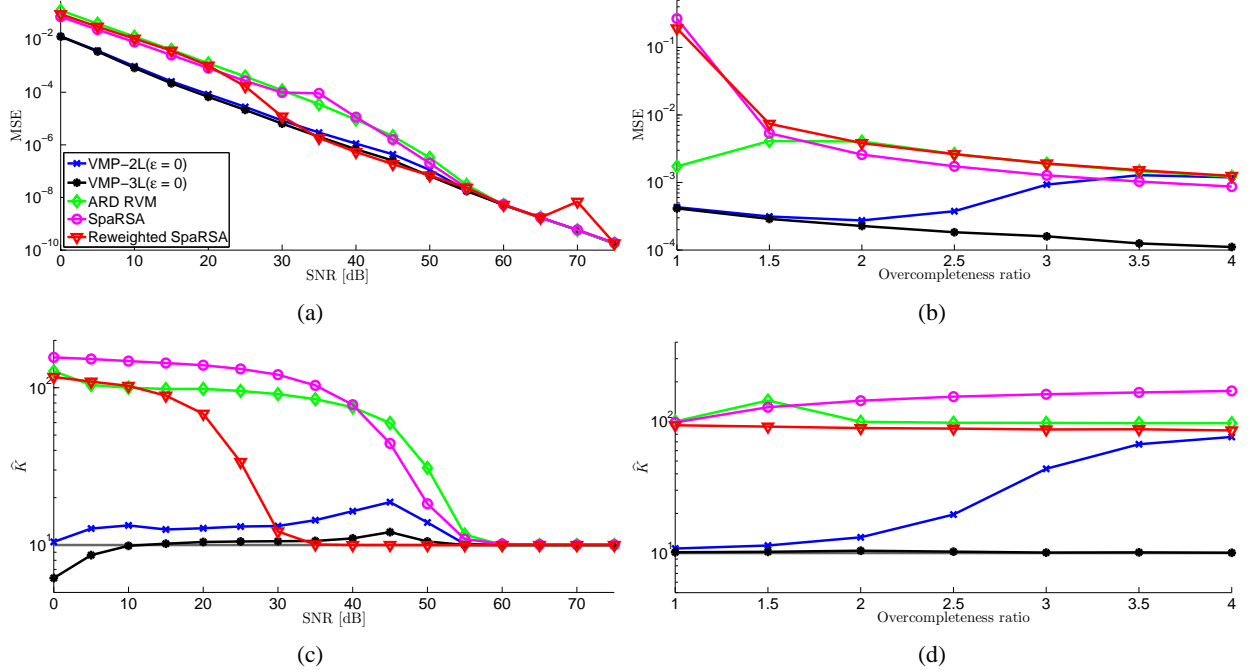


Fig. 8. Performance comparisons of VMP-2L( $\epsilon = 0$ ) and VMP-3L( $\epsilon = 0$ ) with ARD RVM, SparseRSA and Reweighted SparseRSA algorithms: (a,b) MSE versus (a) SNR and (b) overcompleteness ratio  $L/M$  with  $M = 100$ . (c,d) Estimated number of non-zero components  $\hat{K}$  versus (c) SNR and (d) overcompleteness ratio  $L/M$  ( $M=100$ ) at 15 dB SNR. The gray horizontal line indicates the true number of non-zero components in  $\alpha$ .

outperforming VMP-2L( $\epsilon = 0$ ) in terms of the estimated number of non-zero components. A similar trend is observed when the algorithm performance is compared as a function of the overcompleteness ratio  $L/M$  in Figs. 8(b) and 8(d). Although the G-Ga and G-Ga-Ga models with  $\epsilon = 0$  lead to estimators with better performance than the other schemes, the performance of VMP-2L( $\epsilon = 0$ ) degrades as the ratio  $L/M$  increases, while VMP-3L( $\epsilon = 0$ ) performs well almost independently of the actual overcompleteness ratio.

Now we test the performance of the algorithms versus  $K$  with  $L/M = 2$  and  $M = 100$ . The corresponding results are shown in Fig. 9 for the SNR level fixed at 10 dB, 30 dB, and 60 dB. Interestingly, a similar thresholding behavior is observed here also for ARD RVM and both SparseRSA schemes. The VMP schemes perform better in low ( $\sim 10$  dB) and moderate ( $\sim 30$  dB) SNR regimes. In high SNR regime ARD RVM performs almost as well as VMP-2L( $\epsilon = 0$ ), yet it significantly overestimates  $K$  for  $K > 70$ . Reweighted SparseRSA also performs quite well in the high SNR regime, for  $K < 50$ , overestimating  $K$  as  $K$  grows.

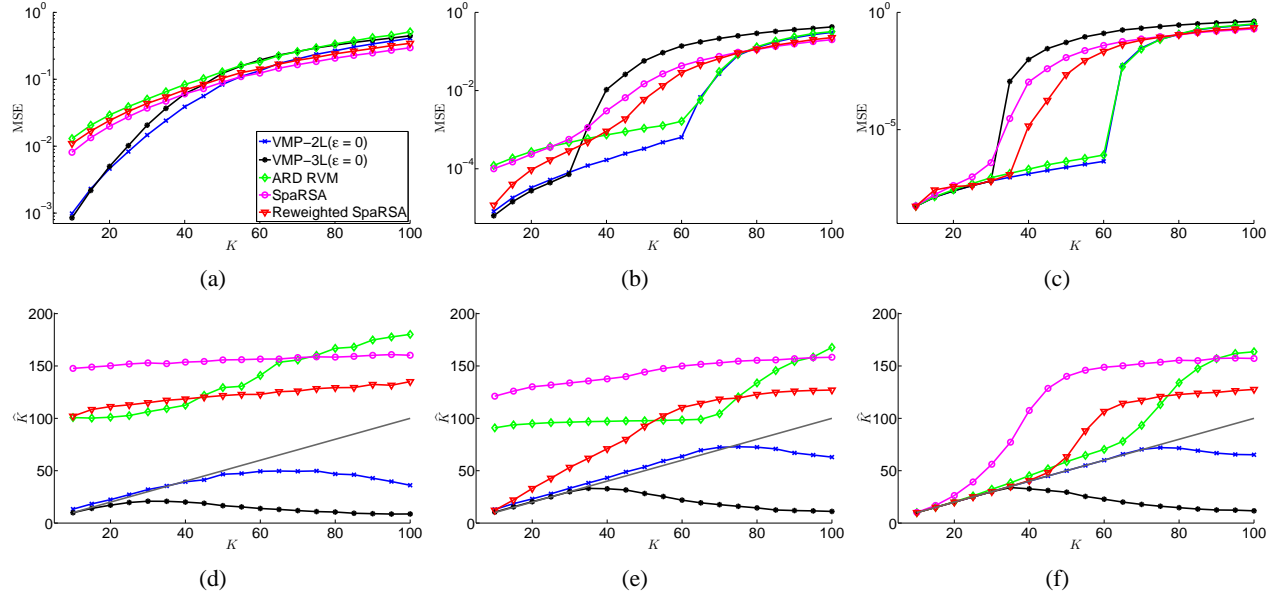


Fig. 9. Performance comparisons of VMP-2L( $\epsilon = 0$ ) and VMP-3L( $\epsilon = 0$ ) with ARD RVM, SparseRSA and Reweighted SparseRSA algorithms: (a)-(c) MSE performance and (d)-(f) estimated number of non-zero components  $\hat{K}$  versus the true number of non-zero components  $K$ . The SNR is set to 10 dB in (a) and (d), 30 dB in (b) and (e), and 60 dB in (c) and (f).

## VI. CONCLUSION

In this paper a unifying sparse Bayesian formalism with hierarchical sparsity prior modeling was proposed. The presented methodology generalizes the sparse modeling of complex- as well as real-valued systems. Taking as a starting point the hierarchical structure for modeling the  $\ell_1$  parameter constraint, originally proposed by M. Figueredo, we extend this model to the complex domain, which leads to a parametric family of sparsity-inducing hierarchical priors.

The new approach uses a product of zero-mean Gaussian priors defined for each element of the parameter vector  $\alpha$ , with the variance of each prior following a gamma distribution characterized by a shape parameter  $\epsilon$  and a component specific scale parameter  $\eta_l$ . This model we termed the Gaussian-gamma prior model. The choice  $\epsilon = 3/2$  in case of complex-valued models and  $\epsilon = 1$  in case of real-valued models corresponds to the Bayesian hierarchical modeling of the  $\ell_1$ -norm constraint in the objective function. Naturally, other values of  $\epsilon \geq 0$  can be utilized. This additional degree of freedom in controlling the sparsity properties with  $\epsilon$  leads to priors with strong sparsity properties. More specifically, it was shown that the case  $\epsilon = 0$  encourages a sparser solution than the  $\ell_1$ -norm constraint. Furthermore, varying the parameter  $\epsilon$  of the Gaussian-gamma model leads to estimators of  $\alpha$  that approximate a well-known soft-thresholding rule.

We also considered a further extension of the Gaussian-gamma prior model by modeling the hyperparameters  $\eta_l$  as random variables with a gamma prior pdf. The new model – the Gaussian-gamma-gamma prior model – also generalizes complex- as well as real-valued scenarios and allows for an automatic selection of the parameter  $\eta_l$ . Similarly to the Gaussian-gamma model, the three-layer Gaussian-gamma-gamma prior also leads to a family of parametric priors with different sparsity-inducing properties. However, varying the free parameters of the Gaussian-gamma-gamma model leads to estimators of  $\alpha$  that approximate a hard-thresholding rule.

Finally, we proposed a variational message passing (VMP) algorithm for the estimation of the model parameters. The proposed VMP algorithm effectively exploits the probabilistic structure of the inference problem. It was shown that in general the case  $\epsilon = 0$  outperforms the  $\ell_1$ -norm constraint both in terms of the sparsity as well as in the achieved MSE. The proposed extension of the Bayesian hierarchical model for sparsity constraint is a very powerful, yet analytically tractable and simple mechanism for implementing sparse estimators. Our numerical results show that we obtained a very significant performance improvement over existing sparse methods when testing in low and moderate SNR regimes, in which state-of-art estimators failed to produce sparse solutions.

## REFERENCES

- [1] R. Baraniuk, “Compressive sensing,” *IEEE Signal Processing Magazine*, vol. 24, no. 4, pp. 118–121, July 2007.
- [2] M. Wakin, “An introduction to compressive sampling,” *IEEE Signal Process. Mag.*, vol. 25, no. 2, pp. 21–30, Mar. 2008.
- [3] D. G. Tzikas, A. C. Likas, and N. P. Galatsanos, “The variational approximation for Bayesian inference,” *IEEE Signal Process. Mag.*, vol. 25, no. 6, pp. 131–146, November 2008.
- [4] W. Bajwa, J. Haupt, A. Sayeed, and R. Nowak, “Compressed channel sensing: A new approach to estimating sparse multipath channels,” *Proceedings of the IEEE*, vol. 98, no. 6, pp. 1058–1076, Jun. 2010.
- [5] D. Shutin and B. H. Fleury, “Sparse variational Bayesian SAGE algorithm with application to the estimation of multipath wireless channels,” *IEEE Trans. on Sig. Proc.*, vol. 59, pp. 3609–3623, 2011.
- [6] D. Shutin, T. Buchgraber, S. R. Kulkarni, and H. V. Poor, “Fast variational sparse Bayesian learning with automatic relevance determination for superimposed signals,” *submitted to IEEE Transactions on Signal Processing*.
- [7] A. Lee, F. Caron, A. Doucet, and C. Holmes, “A hierarchical bayesian framework for constructing sparsity-inducing priors,” Sep. 2010. [Online]. Available: arXiv:1009.1914
- [8] E. J. Candes, M. B. Wakin, and S. P. Boyd, “Enhancing sparsity by reweighted  $\ell_1$  minimization,” *Journal of Fourier Analysis and Applications*, vol. 14, pp. 877–905, 2008.
- [9] M. Seeger and D. Wipf, “Variational bayesian inference techniques,” *Signal Processing Magazine, IEEE*, vol. 27, no. 6, pp. 81 –91, 2010.
- [10] D. Wipf and S. Nagarajan, “Iterative reweighted  $\ell_1$  and  $\ell_2$  methods for finding sparse solutions,” *IEEE Journal of Selected Topics in Signal Processing*, vol. 4, no. 2, pp. 317–329, 2010.

- [11] ——, “A new view of automatic relevance determination,” in *Proc. 21 Annual Conf. on Neural Inform. Process. Systems*. Vancouver, British Columbia, Canada: MIT Press, Dec. 2007.
- [12] M. Tipping, “Sparse Bayesian Learning and The Relevance Vector Machine,” *J. of Machine Learning Res.*, vol. 1, pp. 211–244, June 2001.
- [13] D. Wipf and B. Rao, “Sparse Bayesian learning for basis selection,” *IEEE Trans. on Sig. Proc.*, vol. 52, no. 8, pp. 2153 – 2164, aug. 2004.
- [14] M. E. Tipping and A. C. Faul, “Fast marginal likelihood maximisation for sparse Bayesian models,” in *Proc. 9th International Workshop on Artificial Intelligence and Statistics*, Key West, FL, January 2003.
- [15] D. Shutin, T. Buchgraber, S. R. Kulkarni, and H. V. Poor, “Fast adaptive variational sparse Bayesian learning with automatic relevance determination,” in *Proc. IEEE Int. Conf. Acoustics, Speech, and Signal Processing (ICASSP)*, Prague, Czech Republic, 2011, to appear.
- [16] M. Figueiredo, “Adaptive sparseness for supervised learning,” *IEEE Trans. on Pattern Analysis and Machine Intel.*, vol. 25, no. 9, pp. 1150–1159, 2003.
- [17] R. Tibshirani, “Regression shrinkage and selection via the LASSO,” *J. R. Statist. Soc.*, vol. 58, pp. 267–288, 1994.
- [18] A. Fletcher, S. Rangan, and V. Goyal, “Necessary and sufficient conditions for sparsity pattern recovery,” *IEEE Transactions on Information Theory*, vol. 55, no. 12, pp. 5758 –5772, 2009.
- [19] M. Abramowitz and I. A. Stegun, *Handbook of Mathematical Functions with Formulas, Graphs, and Mathematical Tables*. Dover, 1972.
- [20] P. Moulin and J. Liu, “Analysis of multiresolution image denoising schemes using generalized Gaussian and complexity priors,” *IEEE Transactions on Information Theory*, vol. 45, no. 3, pp. 909–919, 1999.
- [21] D. P. Wipf and S. Nagarajan, “A new view of automatic relevance determination,” *Proc. Neural Information Processing Systems (NIPS)*, vol. 20, 2008.
- [22] E. W. Stacy, “A generalization of the gamma distribution,” *The Annals of Mathematical Statistics*, vol. Vol. 33, no. 3, pp. 1187–1192, Sep. 1962.
- [23] F. R. Kschischang, B. J. Frey, and H. A. Loeliger, “Factor graphs and the sum-product algorithm,” *IEEE Transactions on Information Theory*, vol. 47, no. 2, pp. 498–519, Feb 2001.
- [24] J. Winn and C. M. Bishop, “Variational Message Passing,” *J. Mach. Learn. Res.*, vol. 6, pp. 661–694, 2005.
- [25] B. Jorgensen, *Statistical Properties of the Generalized Inverse Gaussian Distribution (Lecture Notes in Statistics 9)*. Springer-Verlag New York Inc, 1982.
- [26] S. J. Wright, R. D. Nowak, and M. A. T. Figueiredo, “Sparse reconstruction by separable approximation,” *IEEE Trans. on Sig. Proc.*, vol. 57, no. 7, pp. 2479–2493, 2009.